https://doi.org/10.5194/egusphere-2025-1571
Preprint. Discussion started: 10 April 2025

Spatiotemporal properties of intrinsic sea level variability along the Southeast United States coastline

Carmine Donatelli[1], Christopher M. Little[1], Rui M. Ponte[1], Stephen G. Yeager[2]

[1]Atmospheric and Environmental Research, Lexington (MA), USA
[2]National Center for Atmospheric Research, Boulder (CO), USA

Correspondence to: Carmine Donatelli (cdonatelli@aer.com)

Abstract. The influence of intrinsic ocean variability on coastal sea level remains largely unexplored but is of potential importance for emerging forecasting efforts. As in weather forecasts, intrinsic variability will amplify uncertainty in initial conditions. However, variability originating from intrinsic processes may be predictable in a forecast system with sufficient resolution and accurate initialization. Here, we examine the spatiotemporal properties of intrinsic sea level variability along the Southeast United States coast using a suite of global ocean/sea-ice simulations at 0.1° horizontal resolution. In model simulations, intrinsic variability is a dominant component of the monthly de-seasonalized and detrended sea level variability in deep waters, but it is damped along continental shelves, where it comprises ~10-30% of the sea level standard deviation. Our analyses demonstrate that US East Coast and Gulf of Mexico shelves exhibit a common intrinsic mode of sea level variability, with maximal amplitude in the South Atlantic Bight and almost no expression north of Cape Hatteras. This coastal mode is coherent with sea level along the Gulf Stream axis after detachment from Cape Hatteras. Intrinsic sea level variability in the detached Gulf Stream leads the coastal mode by 2-3 months, suggesting that intrinsic coastal sea level variability may exhibit predictability.

Keywords

Sea level, intrinsic variability, United States, shelf-open-ocean connections

1 Introduction

Coastal ecosystems, communities, and economies are highly susceptible to sea level variability over a wide range of time scales (e.g., Leatherman, 2001; Rashid et al., 2021; NOAA, 2022). Accurate predictions are needed for mitigation and adaptation purposes and for effectively managing risks associated with sea level variability. Such predictions will benefit from: 1) improved understanding of relevant drivers of regional coastal sea level variability, and 2) assessment of the capabilities of dynamic models currently utilized in operational ocean forecasting.

Various physical processes operating at different spatial and temporal scales influence sea level variability (e.g., Vinogradov & Ponte, 2011; Gerkema & Duran-Matute, 2017; Little et al., 2019; Camargo et al., 2024). These processes can be partitioned

https://doi.org/10.5194/egusphere-2025-1571
Preprint. Discussion started: 10 April 2025

into a deterministic component that occurs in response to an applied forcing ("atmospherically-forced component" or "forced component"), and a non-deterministic ("intrinsic" or "internal") component, which is not directly driven by atmospheric variability but is instead generated by the ocean itself, for instance, through small-scale (i.e., mesoscale and smaller) turbulent processes (e.g., Penduff et al., 2011). Such small-scale processes become particularly important in eddy-active regions of the ocean and cause the ocean's evolution to be non-deterministic at both small and large (regional to basin) scales under prescribed forcing conditions (Sérazin et al., 2015; Qiu et al., 2015; Forget & Ponte, 2015; Close et al., 2020).

Sea level variability originating from intrinsic processes might be a significant source of uncertainty in forecasts and can only be represented by adopting ocean models of sufficient horizontal resolution (e.g., Penduff et al., 2010; 2011; Sérazin et al., 2018; Chassignet et al., 2020). However, generally, the horizontal resolution of ocean models used for coastal sea level forecasts is on the order of 1° (~100 km), which is insufficient to capture the effect of oceanic intrinsic variability on coastal sea level (e.g., Long et al., 2021).

Even in simulations capable of representing intrinsic processes, separation of forced and intrinsic variability is not trivial. Two strategies have been used to isolate the contribution of intrinsic variability in eddy-permitting ocean model simulations. The first strategy compares model output from a realistic atmospherically forced model with one only subjected to climatological forcing (e.g., Stewart et al., 2020) (i.e., repeat-year forcing simulations). The second approach employs ensemble (i.e., multiple) members with perturbed initial conditions, which permit the estimation of the forced (ensemble mean) and intrinsic components (i.e., difference between time series of a specific member and the ensemble mean) (e.g., Hirschi et al., 2003; Penduff et al., 2014; Bessières et al., 2017).

This paper focuses on characterizing the spatiotemporal properties of intrinsic sea level variability along the Southeast Coast of the United States (including the Gulf of Mexico), where societal vulnerability to sea level variability is high and increasing (e.g., Thatcher et al., 2013). Previous studies indicate regions along the Southeast Coast of the United States (from now on, SEUS) have a strong intrinsic component at sub-annual to interannual timescales (e.g., Close et al., 2020, Little et al. 2024). However, these studies do not elucidate: (i) the SEUS along-coast spatial structure, (ii) the "sources" of continental shelf intrinsic sea level variability in the Gulf of Mexico and the US East Coast, and (iii) how coastal variability relates to offshore variability over space and time. To explore these questions, it is essential to use simulations that: 1) represent the SEUS shelf topography with sufficient grid points even in regions where the shelf narrows, and 2) adequately resolve offshore intrinsic variability (e.g., Halberg et al., 2013).

Here, to study the spatial structure (and magnitude) of intrinsic sea level variability along the SEUS coastline and its spatiotemporal relationship with offshore variability, we utilize monthly sea surface height (SSH) fields from high-resolution (HR) forced ocean/sea-ice (FOSI) and repeat-year-forcing (RYF) (Stewart et al., 2020) simulations performed using the Community Earth System Model at 0.1° horizontal resolution (note the HR RYF simulation cleanly quantifies intrinsic sea level variability) (Chang et al., 2020; Yeager et al., 2023; Little et al., 2024). We also compare sea level hindcasts from the HR FOSI simulation to tide gauge (TG) and altimeter observations over the 1993-2018 period to see if the model faithfully represents coastal and offshore sea levels. The paper is organized as follows. The model setup, observational datasets, and data

https://doi.org/10.5194/egusphere-2025-1571
Preprint. Discussion started: 10 April 2025

processing are described in the Appendix. In Section 2, we show the results, and in Section 3, we present the discussion and conclusions.

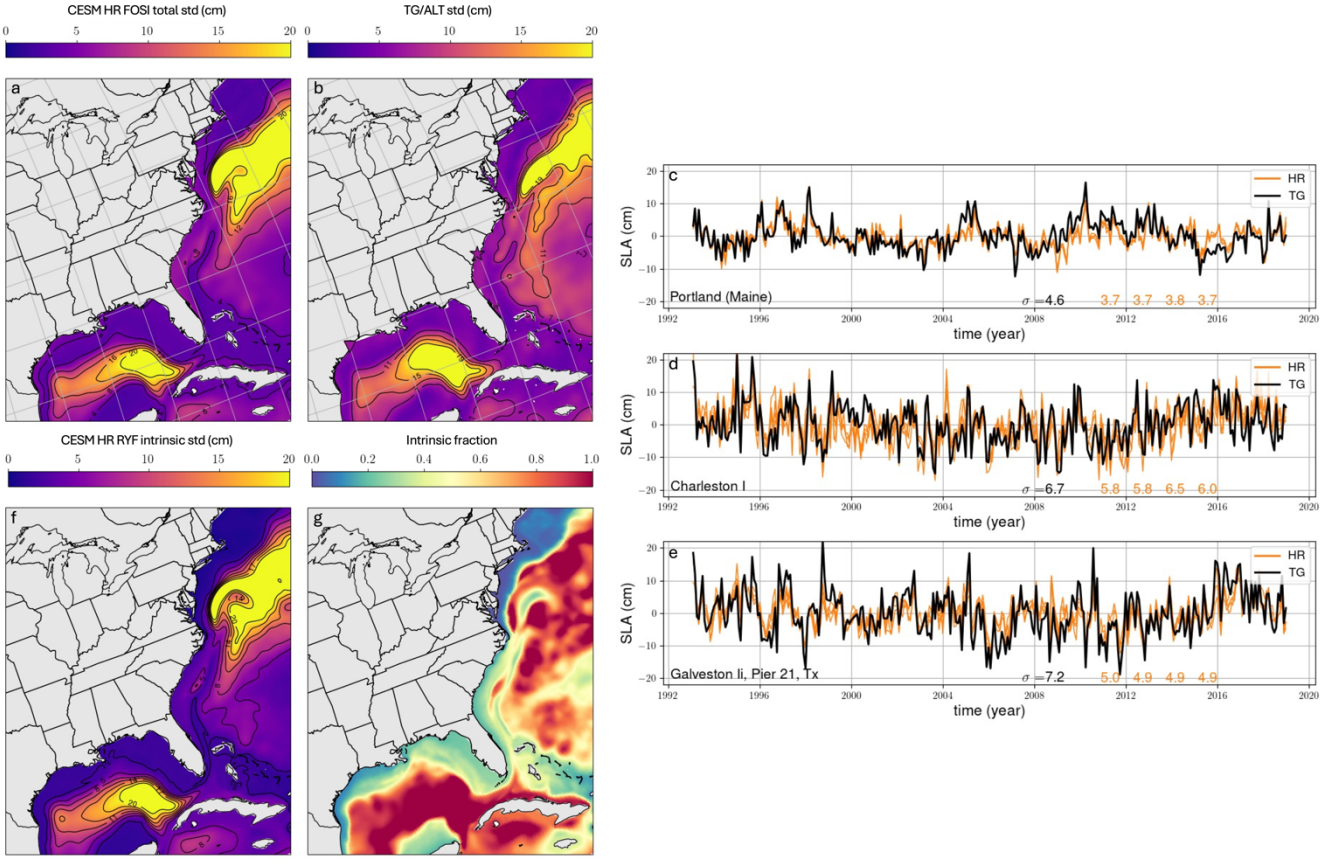

Figure 1: Total sea level standard deviation (cm) from (a) the HR FOSI simulation and (b) gridded altimeter product over the period 1993-2015. (c, d, e) Comparison between detrended and de-seasonalized time series from TGs and HR FOSI ensemble simulation. We reported the standard deviation (cm) for TGs (black) and each FOSI cycle. The location of each TG is shown in Fig. 1b. (f) Intrinsic standard deviation (cm) estimated using the HR RYF simulation. (g) Intrinsic fraction (i.e., intrinsic standard deviation estimated from the HR RYF simulation divided by total standard deviation computed using the HR FOSI simulation).

2 Results

2.1 Total and intrinsic sea level variability

We first compare the total (i.e., forced and intrinsic) sea level standard deviation from the HR FOSI simulation and observations over the 1993-2018 period (Fig. 1). Total sea level standard deviation (mean across the FOSI members; Fig. 1a) is larger in deep waters and decreases over the continental shelf. Over the same temporal window, a gridded altimeter product (Fig. 1b) shows a similar spatial structure, with the model generally underestimating the observed total sea level standard deviation over the shelf by 10-20%. A similar result was obtained when we compared coastal grid points with the detrended

https://doi.org/10.5194/egusphere-2025-1571
Preprint. Discussion started: 10 April 2025

and de-seasonalized sea level recorded by TGs at three representative locations along the US coastline (Figs. 1c, d, e). Discrepancies between model and TG observations were more significant in Galveston. In contrast, Charleston exhibited the largest inter-cycle differences. Our results show that, overall, sea level hindcasts compare favorably to TG and altimeter observations over the 1993-2018 period (see also Little et al., (2024) for model validation).

We next quantify intrinsic variability using detrended and de-seasonalized monthly outputs from the HR RYF simulation (Fig. 1f). The intrinsic standard deviation shows substantial spatial variations; specifically, it is damped on the continental shelf relative to offshore. By computing the intrinsic fraction (i.e., ratio between the intrinsic standard deviation from the HR RYF simulation and the total cycle-mean sea level standard deviation from the HR FOSI simulation), we found that the intrinsic standard deviation represents 10-30% of the total sea level standard deviation on the continental shelf south of Cape Hatteras and up to 100% of the total standard deviation in deep waters (Fig. 1g). Offshore intrinsic variability is maximized in the interior of the Gulf of Mexico and in proximity to the Gulf Stream. Along the Gulf Stream path, we found a minimum in the offshore intrinsic fraction (Fig. 1g), which coincides with a region of low intrinsic standard deviation (Fig. 1f).

2.2 Intrinsic sea level variability along the SEUS coast

We utilized detrended and de-seasonalized monthly SSHs extracted at 170 coastal grid points (pseudo-TGs) from the HR RYF simulation to analyze the spatial structure of intrinsic sea level variability along the SEUS coast. Consistent with Figs. 1f, g, coastal grid points exhibit minimal variability north of Cape Hatters (see pseudo-TGs between locations 100 and 170 in Fig. 2a).

The EOF decomposition revealed that the first two modes explain most of the variability in the dataset. Specifically, the first mode explains 73% of the variability, while the second mode contributes 12% (Figs. 2b, c). The eigenvector associated with the dominant mode showed the same sign in all the pseudo-TGs (as indicated by the color of the circles in Fig. 2b), revealing a “common mode” linking the East Coast and the Gulf of Mexico. In contrast, the second eigenvector suggests that the pseudo-TGs along the US East Coast behave opposite to those in the Gulf of Mexico (Fig. 2c). The variability explained by each mode presents significant spatial variations (see the size of the circles in Figs. 2b, c), particularly between pseudo-TGs south of Cape Hatteras (larger) and those north of Cape Hatteras (smaller standard deviation). Both modes show enhanced variability between Cape Hatteras and Jacksonville.

The temporal evolution of the first two eigenvectors is represented by the PCs associated with each mode (Fig. 2d). Specifically, the PCs exhibit fluctuations at sub-annual to interannual time scales, including significant multi-year sea level trends (for example PC1, over a 5-year period beginning around month 90) (Penduff et al., 2019). The remainder of the paper considers only the first mode (PC1) given its dominant role in explaining SEUS intrinsic coastal variability in the HR RYF simulation.

https://doi.org/10.5194/egusphere-2025-1571
Preprint. Discussion started: 10 April 2025

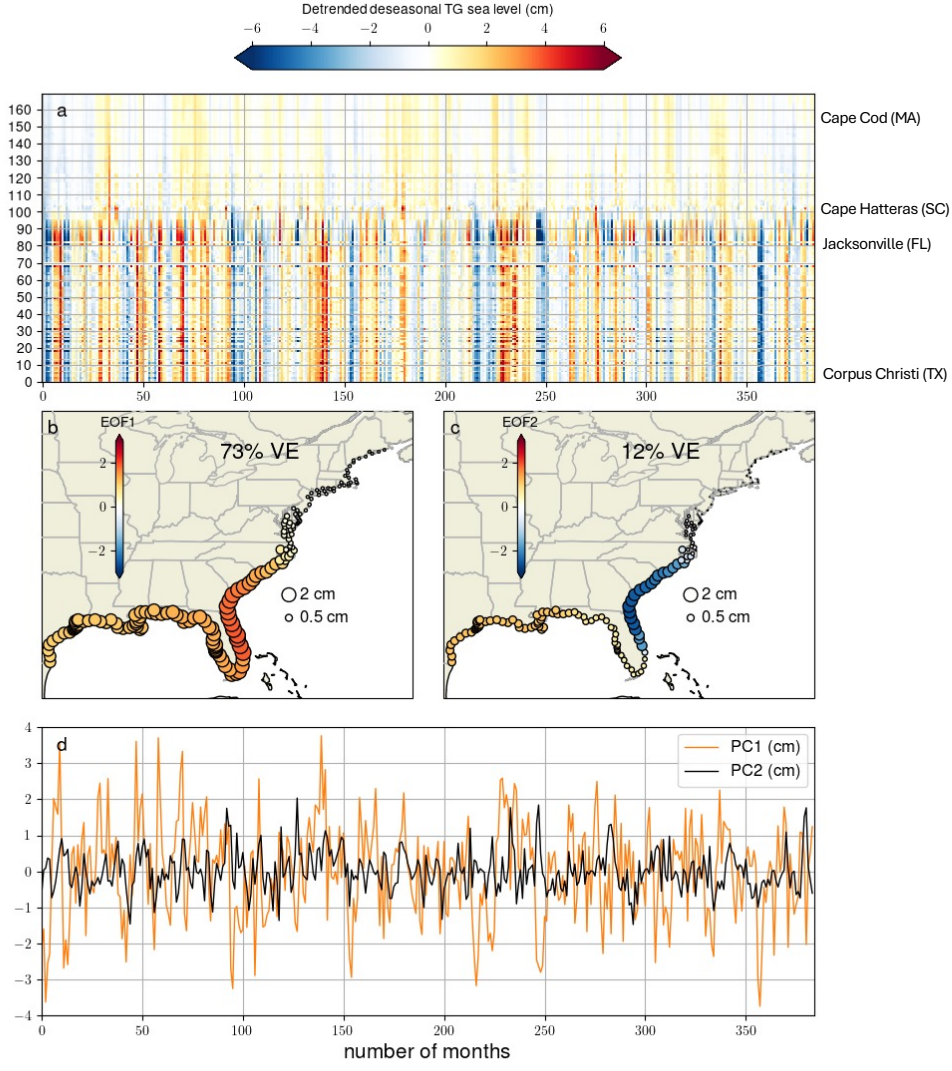

Figure 2: (a) Monthly time series from the HR RYF simulation extracted at 170 pseudo-TGs along the SEUS coastline. These time series are 32 years long. (b) First and (c) second mode obtained from EOF analysis. The color of the circles indicates the eigenvectors' value in each pseudo-TG, while the circles' radius is related to the variability (standard deviation) explained by each mode. (d) Principal components (PCs, cm) associated with modes 1 and 2.

2.3 Relationship between along-coast and offshore intrinsic sea level variability

We utilized detrended and de-seasonalized SSH fields obtained from the HR RYF simulation to identify spatial pathways connecting offshore and coastal intrinsic sea level variability. With no lag, PC1 correlates with (i) SSHs over the entire continental shelf south of Cape Hatteras, and (ii) SSHs within an off-shelf region located in proximity to the Gulf Stream axis after detachment from Cape Hatteras (Fig. 3a).

https://doi.org/10.5194/egusphere-2025-1571
Preprint. Discussion started: 10 April 2025

To assess evidence for propagating oceanic signals, lag correlations at different lags (i.e., 3 months, 1 month, and -1 month) were applied, with a positive lag indicating that offshore sea level leads PC1. We highlight significantly correlated off-shelf regions using a threshold of 0.3 (blue contours in Figs. 3b, c, d). Interestingly, lag correlations reveal that the off-shelf region (i) moves westward and varies in size with decreasing time lag, and (ii) leads the along-coast intrinsic mode. Although partially overlapping, the detected offshore regions (Fig. 3) and the minimum in the offshore intrinsic fraction in Fig. 1g do not represent the same area. Specifically, the offshore regions in Fig. 3 are displaced northward compared to the minimum in the offshore intrinsic fraction (Fig. 1g).

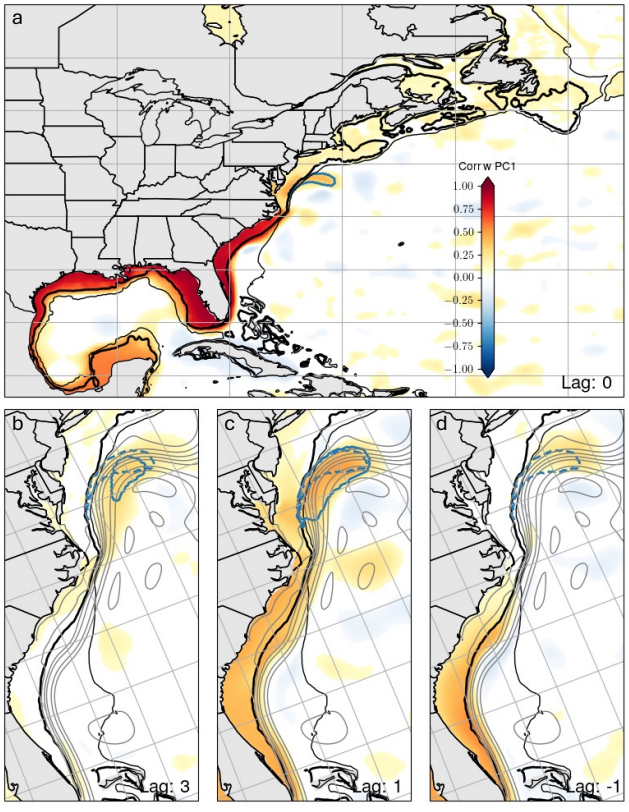

Figure 3: Lag correlations between the PC1 and SSH field: (a) no lag, (b) lag of 3 months, (c) lag of 1 month, and (d) lag of -1 month. A positive lag means that SSH field leads the PC1. The solid blue line in 3a shows the off-shelf region when no lag is applied to the PC1. The solid lines in 3b, c represent the off-shelf region when lags of (b) 3 months and (c) 1 month are applied to the PC1. The dashed lines in 3b, c, and d show the off-shelf region when no lag is applied to the PC1 (i.e., the dashed lines are the same as the solid line in 3a). The statistical significance of the lag correlations was evaluated using a *p-value* of 0.05. The thicker black lines indicate a water depth of 100 meters, while the lighter black line indicates a water depth of 1000 meters. The grey lines are time-mean SSH contours at 10-cm intervals.

We employed a spectral approach to further characterize the relationship between the PC1 and the detrended and de-seasonalized SSHs over the off-shelf region (i.e., solid blue line in Fig. 3a). The two-time series show high coherence values (coherence amplitude greater than 0.5, Fig. 4a) for frequencies smaller than 0.9 year^{-1}. In this frequency band, the coherence

https://doi.org/10.5194/egusphere-2025-1571
Preprint. Discussion started: 10 April 2025

phase lag (positive phase lag denotes off-shelf region leads the PC; shown only for frequency bands where coherence is statistically significant) ranges between 20 and 40 degrees (i.e., off-shelf region leads PC1 by 2-3 months). To help visualize these results, we applied a 13-month low-pass filter to the two-time series (Fig. 4b). Consistent with Fig. 4a, the two filtered signals show that the off-shelf region leads the along-coast intrinsic mode.

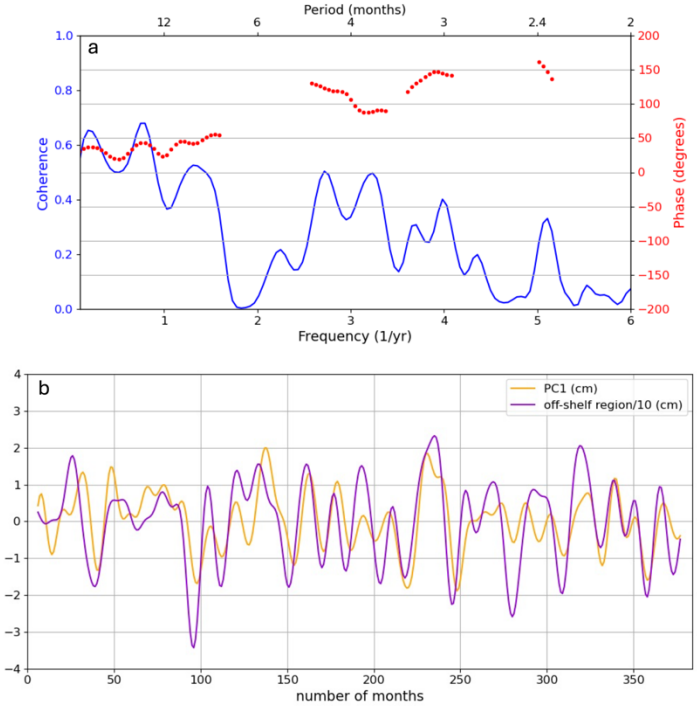

Figure 4: (a) Coherence analysis between the PC1 and average SSH signal within the off-shelf region. Note phase lag is only shown for statistically significant coherence (a positive phase means that the off-shelf region leads the PC1). (b) PC1 (cm) and average SSH signal (cm) within the off-shelf region to which we applied a 13-month low-pass filter. The average SSH signal within the off-shelf region is divided by 10.

3 Discussion and Conclusions

Using a 50-member ocean ensemble hindcast at 0.25° horizontal resolution, Close et al. (2020) showed that sea level variability is almost entirely driven by intrinsic processes in energetic regions of the ocean, such as the Gulf Stream (GS) and the Gulf of Mexico Loop Current. Building on this study, we utilized a set of numerical experiments at higher spatial resolution to explore the linkage between offshore and coastal sea level variability along the SEUS coastline.

Our analyses revealed that, at monthly to interannual timescales south of Cape Hatteras for the 1993-2018, intrinsic processes meaningfully contribute to sea level variability, reaching up to 30% of the total monthly sea level standard deviation on the continental shelf. A common intrinsic sea level mode, largest between Charleston and the Florida Straits, but coherent around the Gulf of Mexico, is correlated with sea level variability in the detached GS. The absence of intrinsic variability to the north

https://doi.org/10.5194/egusphere-2025-1571
Preprint. Discussion started: 10 April 2025

of Cape Hatteras is consistent with the limited ability of eddies to influence sea level where the shelf is wide (e.g., Gangopadhyay et al., 2020), and the equatorward propagation of coastal sea level anomalies originating near the GS detachment.

While we leave a detailed examination of the dynamics underlying the offshore sea level variability and its communication to the coast for future work, the along-coast coherence of PC1, and the robust 2-3 month lag (Fig. 4), inform hypotheses about the underlying oceanic mechanisms. The propagation of sea level anomalies from the off-shelf region to Cape Hatteras might occur along the slope via topographic Rossby waves (e.g., Wise et al., 2018; Hughes et al., 2019; Wise et al., 2020). The latter travel with a speed of a few centimeters per second at these latitudes (first baroclinic mode), roughly consistent with the time lag we quantified between the off-shelf region and the PC1 (it should be noted that barotropic Rossby waves may also be involved in this transfer process). Once on the shelf, sea level anomalies are transmitted via Kelvin waves traveling at a few meters per second (first baroclinic mode); such signals can travel from Cape Hatteras to the Gulf of Mexico in less than a month. This lag is not resolved using the monthly SSH fields available from the HR RYF and is thus consistent with our identification of a single signed coastal mode. Given the disparity between open-ocean and coastal wave speeds, SSH fields at higher temporal resolution will be required to capture the along-coast propagation of sea level anomalies.

Future investigations are also needed to shed light on the nature of sea level variability in the off-shelf region. This region might be related to the demise location of warm-core eddies (WCRs) (e.g., Gangopadhyay et al., 2020). However, the frequency band in which the along-coast intrinsic mode and the off-shelf region exhibit high coherence (i.e., frequencies smaller than 0.9 $year^{-1}$) suggests that SSH within the off-shelf region might also be influenced by physical mechanisms that are not linked to the individual WCRs' demise, whose typical frequency is likely larger than 0.9 $year^{-1}$ (e.g., Silva et al., 2020). These mechanisms may include, among others, variations in the GS position excited by intrinsic oceanic variability (e.g., Quattrocchi et al., 2012; Gregorio et al., 2015). More specifically, frequencies smaller than 0.9 $year^{-1}$ seem consistent with interannual GS path oscillations, which are known to control a significant fraction of the total SSH variance within the GS detachment region (e.g., Guo et al., 2023). Related to this point, it is important to mention that the GS is often misplaced in numerical models (Chassignet & Marshall, 2008). As shown in Chassignet et al. (2020), this GS separation bias produces excessive surface EKE north of Cape Hatteras in POP (Parallel Ocean Program, Smith et al., (2010)) HR FOSI and, therefore, we can expect that it may also impact the magnitude of the along-coast mode detected in the HR RYF simulation.

Although further studies are required to assess the representation of this mode in models (and observations, if isolation of intrinsic variability is possible), CESM simulations suggest that intrinsic sea level variability is smaller (in a time-aggregated sense) than forced sea level variability; however, it is not negligible and, as noted, may have inherent predictability. We thus suggest that sea level forecasting efforts will benefit from further studies of intrinsic variability along the SEUS coastline and elsewhere. Furthermore, the ocean mechanisms involved in the communication of off-shelf anomalies to the coast (and from Cape Hatteras to the Gulf of Mexico) are likely the same as those regulating the transfer of other sea-level signals, regardless of their forced or intrinsic nature. As such, our findings can help provide a better understanding of (i) the physical processes governing offshore-shelf and shelf-to-shelf communication along the SEUS coastline and (ii) the GS effects on coastal sea

https://doi.org/10.5194/egusphere-2025-1571
Preprint. Discussion started: 10 April 2025

level (e.g., Ezer, 1995; Ezer et al., 2013). Targeted experiments might also address questions outside the scope of this study, including potential interactions between forced and intrinsic variability.

Appendix A. CESM simulations

We employed an HR FOSI simulation with a spatial resolution of 0.1° (~10 km) to analyze monthly SSH fields from 1993 to 2018. Simulations were performed using the global Community Earth System Model version 1.3 (CESM1.3) following the Ocean Model Intercomparison Project version 2 (OMIP2) experimental protocol (Griffies et al., 2016). The 1958-2018 forcing applied is (nearly) identical in each of four consecutive cycles and is obtained from JRA55 reanalysis. The JRA55 atmospheric fields have a spatial resolution of 55 km and a temporal resolution of 3 hours. The HR FOSI simulation was initialized from observed climatology (i.e., World Ocean Atlas) and spun up through consecutive cycles of 1958-2018 (61-year) forcing. Each cycle repeats the forcing of the previous simulation (e.g., simulation years 62-122 (cycle 2) repeats the forcing of simulation years 1-61 (cycle 1)). Since the cycles share the same forcing but have different initial conditions, inter-cycle differences can be largely attributed to intrinsic processes.

The limited number of HR FOSI cycles does not allow a clear separation of forced and intrinsic variability (although estimation of the forced and intrinsic variance might be possible using inter-cycle differences, see Little et al. (2024)). To cleanly quantify intrinsic variability, we use an HR RYF simulation. The HR RYF simulation was carried out by applying a single year of JRA55 boundary conditions (May 2003 to the end of April 2004). Here, we analyzed the last 32 years of monthly outputs from a 70-year-long HR RYF simulation to examine the spatiotemporal properties of intrinsic sea level variability along the SEUS coastline, over the continental shelf, and adjacent deep waters. Further details of the model setup can be found in Little et al. (2024).

Appendix B. Observational dataset and comparisons with model outputs

We utilized monthly mean TG observations with less than 12 missing months over the 1993-2018 period. TG observations were obtained from the Permanent Service for Mean Sea Level Revised Local Reference database on December 1, 2022 (Holgate et al., 2013). Missing data were infilled using linear interpolation after removing the seasonal cycle from the time series.

Sea level recorded by TGs is affected by numerous processes not accounted for in CESM simulations (e.g., inverted barometer effect, barystatic changes, global mean steric expansion/contraction, and vertical land motion). Thus, we removed from the TG record (i) the inverted barometer effect, using surface pressure fields from the ERA-5 atmospheric reanalysis, and (ii) the global mean sea level due to barystatic and steric processes, employing estimates obtained from altimetry (MeaSUREs, 2021). Additionally, we linearly detrended the corrected TG time series to account for vertical land motion (after correction and detrending, we denote sea level as ζ').

To compare model output and sea level observed by TGs, we extracted the SSH in the closest model grid points to each TG using a ball tree algorithm. The modelled time series were detrended to remove model drift. To evaluate the model performance

https://doi.org/10.5194/egusphere-2025-1571
Preprint. Discussion started: 10 April 2025

at larger spatial scales, we compared the spatial structure of ζ' variability from the HR FOSI simulation with a 1/6° gridded satellite altimeter product at monthly temporal resolution over the 1993-2018 period (MeaSUREs, 2022). Before comparing the two datasets, we removed the global mean sea level and linearly detrended the residual at each grid point from the altimeter product (note that the inverted barometer effect has already been removed from the altimeter gridded product).

Appendix C. Additional data processing

SSH time series were extracted from the HR RYF simulation along the SEUS coast at 170 pseudo-TGs (one pseudo-TG for each model grid cell along the coast). Then, we applied Empirical Orthogonal Function (EOF) analysis on the extracted SSH time series to identify the modes that explain the largest fraction of variability in the dataset. First, a matrix (O) was created by storing the time series extracted from the HR RYF simulation along each column. Then, we computed the covariance matrix ($C = O^T O$) and solved the corresponding eigenvalue problem:

$$C = V\lambda V^T \quad \text{(C1)}$$

where V and λ are the eigenvector and eigenvalue matrices. Each eigenvalue indicates the fraction of the variance explained by each eigenvector. By expressing matrix O in the space identified by the eigenvectors, we computed the principal components (PCs) associated with each mode.

We also utilized coherence analysis to characterize the relationship between along-coast and offshore intrinsic sea level variability. The spectrum was obtained by applying a Hanning window with overlapping (50% overlap) data segments. Each data segment has a length of 64 time steps (i.e., 64 months) and starts halfway through the previous segment (i.e., each data segment captures half of the data of the previous one). Coherence uncertainties were obtained using a standard approach (e.g., Gallet & Julien, 2011). This approach sets a threshold to assess whether a computed coherence exceeds what might be expected from random noise. The threshold is determined based on the significance level (i.e., 95% significance level) and the number of segments used to compute the coherence spectrum. The number of segments was evaluated as the time series length divided by the window length multiplied by 0.5.

Data availability

Sea level observations analyzed in this study are available from the Permanent Service for Mean Sea Level (Holgate et al., 2013; Permanent Service for Mean Sea Level, 2024) (for tide gauges) and from NASA (MEaSUREs, 2021) (for satellite altimetry). Derived quantities from CESM simulations, and scripts required to generate figures, are archived at Little (2024).

Author contribution

CD and CML conceptualized the study and performed the analyses. CD wrote the original draft. SGY ran the numerical simulations. CML, RMP, and SGY edited the draft and acquired funding.

https://doi.org/10.5194/egusphere-2025-1571
Preprint. Discussion started: 10 April 2025

Competing interests

The authors declare that they have no conflict of interest.

Acknowledgements

(Reviewers will be acknowledged).
NCAR computational resources were used for data and model analysis; NCAR is a major facility sponsored by the NSF under Cooperative Agreement 1852977. We thank the Permanent Service for Mean Sea Level and the developers of the momlevel Python package (https://momlevel.readthedocs.io/en/v0.0.7/). Maps were generated using python 3.8 (http://www.python.org), matplotlib 3.7.3 (https://matplotlib.org/), and cartopy 0.21.1 (https://scitools.org.uk/cartopy).

Financial support

C.L. and S.Y. acknowledge support from NOAA Climate Program Office NA23OAR4310458. S.Y. acknowledges partial support from the National Academies of Science and Engineering Gulf Research Program grant 2000013283. R.P. acknowledges support from the National Science Foundation Physical Oceanography Program grant OCE-2239805.

https://doi.org/10.5194/egusphere-2025-1571
Preprint. Discussion started: 10 April 2025

References

Bessières, L., Leroux, S., Brankart, J-M., Molines, J.-M., Moine, M.-P., Bouttier, P.-A., Penduff, T., Terray, L., Barnier, B., Sérazin, G., (2017). Development of a probabilistic ocean modelling systembased on NEMO 3.5: application at eddying resolution. Geosci Model Dev 10:1091-1106. https://doi.org/10.5194/gmd-10-1091-2017

Camargo, C. M., Piecuch, C. G., & Raubenheimer, B. (2024). From Shelfbreak to Shoreline: Coastal sea level and local ocean dynamics in the Northwest Atlantic. Geophysical Research Letters, 51(14), e2024GL109583

Chang, P., Zhang, S., Danabasoglu, G., Yeager, S. G., Fu, H., Wang, H., ... & Wu, L. (2020). An unprecedented set of high-resolution earth system simulations for understanding multiscale interactions in climate variability and change. Journal of Advances in Modeling Earth Systems, 12(12), e2020MS002298

Chassignet, E. P., Yeager, S. G., Fox-Kemper, B., Bozec, A., Castruccio, F., Danabasoglu, G., . . . Xu, X. (2020). Impact of horizontal resolution on global ocean–sea ice model simulations based on the experimental protocols of the Ocean Model Intercomparison Project phase 2 (OMIP-2). Geosci. Model Dev., 13(9), 4595–4637. Retrieved from https://gmd.copernicus.org/articles/13/4595/2020/ (Publisher: Copernicus Publications) doi: 10.5194/gmd-13-4595-2020

Close, S., Penduff, T., Speich, S., & Molines, J.-M. (2020). A means of estimating the intrinsic and atmospherically-forced contributions to sea surface height variability applied to altimetric observations. 184, 102314. Retrieved 2023-03-11, from https://linkinghub.elsevier.com/retrieve/pii/S0079661120300537 doi: 10.1016/j.pocean.2020.102314

Ezer, T., Mellor, G. L., and Greatbatch, R. J. (1995). On the interpentadal variability of the North Atlantic Ocean: Model simulated changes in transport, meridional heat flux and coastal sea level between 1955–1959 and 1970–1974. Journal of Geophysical Research: Oceans, 100(C6), 10559-10566

Ezer, T., Atkinson, L. P., Corlett, W. B., and Blanco, J. L. (2013). Gulf Stream's induced sea level rise and variability along the US mid-Atlantic coast. Journal of Geophysical Research: Oceans, 118(2), 685-697

Forget, G., & Ponte, R. M. (2015). The partition of regional sea level variability. Progress in Oceanography, 137, 173-195

Gallet, C., & Julien, C. (2011). The significance threshold for coherence when using the Welch's periodogram method: Effect of overlapping segments. Biomedical Signal Processing and Control, 6(4), 405-409

Gerkema, T., & Duran-Matute, M. (2017). Interannual variability of mean sea level and its sensitivity to wind climate in an inter-tidal basin. Earth System Dynamics, 8(4), 1223-1235

https://doi.org/10.5194/egusphere-2025-1571
Preprint. Discussion started: 10 April 2025

Gopal, A. (2022). The Impact of Horizontal Resolution on Projected Sea-Level Rise Along US East Continental Shelf With the Community Earth System Model. Journal of Advances in Modeling Earth Systems, 14(5). Retrieved 2022-05-18, from https://onlinelibrary.wiley.com/doi/10.1029/ 2021MS002868 doi: 10.1029/2021MS002868

Grégorio, S., Penduff, T., Sérazin, G., Molines, J. M., Barnier, B., & Hirschi, J. (2015). Intrinsic variability of the Atlantic meridional overturning circulation at interannual-to-multidecadal time scales. Journal of Physical Oceanography, 45(7), 1929-1946

Griffies, S. M., Danabasoglu, G., Durack, P. J., Adcroft, A. J., Balaji, V., Böning, C. W., . . . Yeager, S. G. (2016). OMIP contribution to CMIP6: experimental and diagnostic protocol for the physical component of the Ocean Model Intercomparison Project. Geoscientific Model Development, 9(9), 3231– 3296. Retrieved 2018-06-27, from http://www.geosci-model-dev.net/9/ 3231/2016/ doi: 10.5194/gmd-9-3231-2016

Guo, Y., Bishop, S., Bryan, F., & Bachman, S. (2023). Mesoscale variability linked to interannual displacement of Gulf Stream. Geophysical Research Letters, 50(7), e2022GL102549

Hallberg, R. (2013). Using a resolution function to regulate parameterizations of oceanic mesoscale eddy effects. Ocean Modelling, 72, 92-103

Hirschi, J., Baehr, J., Marotzke, J., Stark, J., Cunningham, S., & Beismann, J. O. (2003). A monitoring design for the Atlantic meridional overturning circulation. Geophysical Research Letters, 30(7)

Holgate, S. J., Matthews, A., Woodworth, P. L., Rickards, L. J., Tamisiea, M. E., Bradshaw, E., . . . Pugh, J. (2013). New Data Systems and Products at the Permanent Service for Mean Sea Level. Journal of Coastal Research, 29 (3), 493–504. doi:10.2112/JCOASTRES-D-12-00175.1

Hughes, C. W., Fukumori, I., Griffies, S. M., Huthnance, J. M., Minobe, S., Spence, P., . . . Wise, A. (2019). Sea Level and the Role of Coastal Trapped Waves in Mediating the Influence of the Open Ocean on the Coast. Surveys in Geophysics, 40 (6), 1467–1492. Retrieved 2020-02- 18, from http://link.springer.com/10.1007/s10712-019-09535-x doi: 10.1007/s10712-019-09535-x

Huthnance, J. M. (2004). Ocean-to-shelf signal transmission: A parameter study. Journal of Geophysical Research, 109(C12). Retrieved 2018-10- 20, from http://doi.wiley.com/10.1029/2004JC002358 doi: 10.1029/ 2004JC002358

https://doi.org/10.5194/egusphere-2025-1571
Preprint. Discussion started: 10 April 2025

Leatherman, S. P. (2001). Social and economic costs of sea level rise. In *International Geophysics* (Vol. 75, pp. 181-223). Academic press.

Li, D., Chang, P., Yeager, S. G., Danabasoglu, G., Castruccio, F. S., Small, J., . . . Gopal, A. (2022). The Impact of Horizontal Resolution on Projected Sea-Level Rise Along US East Continental Shelf with the Community Earth System Model. Journal of Advances in Modeling Earth Systems, 14(5). Retrieved 2022-05-18, from https://onlinelibrary.wiley.com/doi/10.1029/2021MS002868 doi: 10.1029/2021MS002868

Little, C. M., Hu, A., Hughes, C. W., McCarthy, G. D., Piecuch, C. G., Ponte, R. M., & Thomas, M. D. (2019). The Relationship Between U.S. East Coast Sea Level and the Atlantic Meridional Overturning Circulation: A Review. Journal of Geophysical Research: Oceans, 124 (9), 6435–6458. Retrieved 2020-08-14, from https://onlinelibrary.wiley.com/doi/abs/10.1029/2019JC015152 doi: 10.1029/2019JC015152

Little, C.M., Yeager, S.G., Ponte, R.M., et al. (2024). Influence of ocean model horizontal resolution on the representation of global annual-to-multidecadal coastal sea level variability. ESS Open Archive. doi: 10.22541/essoar.172374117.76798032/v1

Long, X., Widlansky, M. J., Spillman, C. M., Kumar, A., Balmaseda, M., Thompson, P. R., et al. (2021). Seasonal forecasting skill of sea-level anomalie in a multi-model prediction framework. Journal of Geophysical Research: Oceans, 126, e2020JC017060. https:// doi.org/10.1029/2020JC017060

MEaSUREs. (2021). Global Mean Sea Level Trend from Integrated Multi-Mission Ocean Altimeters TOPEX/Poseidon, Jason-1, OSTM/Jason-2, and Jason-3 Version 5.1. NASA Physical Oceanography DAAC. Retrieved from https://podaac.jpl.nasa.gov/dataset/MERGED TP J1 OSTM OST GMSL ASCII V51 doi: 10.5067/GMSLM-TJ151

MEaSUREs. (2022). MEaSUREs Gridded Sea Surface Height Anomalies Version 2205. NASA Physical Oceanography DAAC. Retrieved from https://podaac.jpl.nasa.gov/dataset/SEA SURFACE HEIGHT ALT GRIDS L4 2SATS 5DAY 6THDEG V JPL2205 doi: 10.5067/SLREF-CDRV3

NOAA. (2022). A NOAA capability for Coastal Flooding and Inundation Information and Services at Climate Timescales to Reduce Risk and Improve Resilience. Retrieved from https://cpo.noaa.gov/Portals/0/ Docs/Risk-Teams/NOAA-Coastal-Inundation-at-Climate-Timescales -Whitepaper.pdf

Penduff, T., Juza, M., Brodeau, L., Smith, G. C., Barnier, B., Molines, J.-M., . . . Madec, G. (2010). Impact of global ocean model resolution on sea-level variability with emphasis on interannual time scales. Ocean Sci., 6(1), 269–284. Retrieved 2014-05-23, from http://www.ocean-sci.net/6/269/ 2010/ (bibtex: penduff2010) doi: 10.5194/os-6-269-2010

https://doi.org/10.5194/egusphere-2025-1571
Preprint. Discussion started: 10 April 2025

Penduff, T., Juza, M., Barnier, B., Zika, J., Dewar, W. K., Treguier, A.-M., . . . Audiffren, N. (2011). Sea Level Expression of Intrinsic and Forced Ocean Variabilities at Interannual Time Scales. Journal of Climate, 24(21), 5652–5670. Retrieved 2023-03-11, from http://journals.ametsoc.org/doi/ 10.1175/JCLI-D-11-00077.1 doi: 10.1175/JCLI-D-11-00077.1

Penduff, T., Barnier, B., Terray, L., Bessières, L., Sérazin, G., Gregorio, S., ... & Brasseur, P. (2014). Ensembles of eddying ocean simulations for climate. CLIVAR Exchanges, Special Issue on High Resolution Ocean Climate Modelling, 19

Penduff, T., Llovel, W., Close, S. et al. (2019). Trends of Coastal Sea Level Between 1993 and 2015: Imprints of Atmospheric Forcing and Oceanic Chaos. Surv Geophys 40, 1543–1562. https://doi.org/10.1007/s10712-019-09571-7
Permanent Service for Mean Sea Level (PSMSL), 2024, "Tide Gauge Data", Retrieved 09 Sep 2024 from http://www.psmsl.org/data/obtaining/

Quattrocchi, G., Pierini, S., and Dijkstra, H. A. (2012). Intrinsic low-frequency variability of the Gulf Stream, Nonlin. Processes Geophys., 19, 155–164, https://doi.org/10.5194/npg-19-155-2012

Qiu, B., Chen, S., Wu, L., and Kida, S. (2015). Wind-versus eddy-forced regional sea level trends and variability in the North Pacific Ocean. Journal of Climate, 28(4), 1561-1577

Rashid, M. M., Wahl, T., & Chambers, D. P. (2021). Extreme sea level variability dominates coastal flood risk changes at decadal time scales. *Environmental Research Letters*, *16*(2), 024026

Sérazin, G., Penduff, T., Gregorio, S., Barnier, B., Molines, J.-M., & Terray, L. (2015). Intrinsic Variability of Sea Level from Global Ocean Simulations: Spatiotemporal Scales. Journal of Climate, 28(10), 4279–4292. Retrieved 2018-06-27, from http://journals.ametsoc.org/doi/10.1175/ JCLI-D-14-00554.1 doi: 10.1175/JCLI-D-14-00554.1

Sérazin, G., Penduff, T., Barnier, B., Molines, J. M., Arbic, B. K., Müller, M., & Terray, L. (2018). Inverse cascades of kinetic energy as a source of intrinsic variability: A global OGCM study. Journal of Physical Oceanography, 48(6), 1385-1408

Smith, R., Jones, P., Briegleb, B., Bryan, F., Danabasoglu, G., Den- nis, J., Dukowicz, J., Eden, C., Fox-Kemper, B., Gent, P., Hecht, M., Jayne, S., Jochum, K. L. M., Large, W., Maltrud, M., Nor- ton, N., Peacock, S., Vertenstein, M., and Yeager, S. (2010). The parallel ocean program (POP) reference manual: ocean component of the community climate system model (CCSM) and community earth system model (CESM), Rep. LAUR-01853, 141, 1–140

Thatcher, C. A., Brock, J. C., & Pendleton, E. A. (2013). Economic vulnerability to sea-level rise along the northern US Gulf Coast. *Journal of Coastal Research*, (63), 234-243

https://doi.org/10.5194/egusphere-2025-1571
Preprint. Discussion started: 10 April 2025

Vinogradov, S. V., & Ponte, R. M. (2011). Low-frequency variability in coastal sea level from tide gauges and altimetry. Journal of Geophysical Research, 116(C7). Retrieved 2018-06-27, from http://doi.wiley.com/10.1029/ 2011JC007034 doi: 10.1029/2011JC007034

Wise, A., Hughes, C. W., & Polton, J. A. (2018). Bathymetric Influence on the Coastal Sea Level Response to Ocean Gyres at Western Boundaries. Journal of Physical Oceanography, 48 (12), 2949–2964. Retrieved 2019-03-07 from http://journals.ametsoc.org/doi/10.1175/JPO-D-18-0007.1 doi: 10.1175/JPO-D-18-0007.1

Wise, A., Polton, J. A., Hughes, C. W., & Huthnance, J. M. (2020). Idealised modelling of offshore-forced sea level hot spots and boundary waves along the North American East Coast. Ocean Modelling, 155, 101706. Retrieved 2020-10-19, from https://linkinghub.elsevier.com/retrieve/pii/S1463500320302080 doi: 10.1016/j.ocemod.2020.101706

Yeager, S. G., Chang, P., Danabasoglu, G., Rosenbloom, N., Zhang, Q., Castruccio, F. S., ... and Simpson, I. R. (2023). Reduced Southern Ocean warming enhances global skill and signal-to-noise in an eddy-resolving decadal prediction system. npj Climate and Atmospheric Science, 6(1), 107